NanoSteels
(The Newest Approaches Toward the Training and Applications of Nanotechnology in Mass Production of Nanostructure Steels)

Shahram Ahmadi[1], Hamid Reza Shahverdi[2] and Ali Shokuhfar[3]

Abstract : The term NanoSteels is called to some special steels consisting of nanosize phases (i.e. ferrite, cementite, and austenite), grains, and carbides (e.g. vanadium and M_2C) produced by nanotechnology. It is proof that exotic physical, mechanical, and magnetic properties can be obtained from nanostructured steels. Fabrication methods of nanostructure steels can be divided into two main categories, SPD (severe plastic deformation) and melt base (crystallization from amorphous state) methods. Among all of the severe plastic deformation techniques (i.e. ECAP, HPT, and ARB), equal channel angular pressing (ECAP) is especially attractive because it can economically produce bulk of ultra- fine grain (UFG) materials. On the other hand, crystallization from amorphous state in bulk metallic glasses is a unique approach toward the mass production of nanostructure ferrous alloys. In the experimental process, crystallization of α – Fe phase during annealing process of $Fe_{55}Cr_{18}Mo_7B_{16}C_4$ bulk amorphous alloy has been evaluated by X- ray diffraction and TEM observations. It is known from the TEM observations that crystalline α – Fe phase nucleated in the structure of the alloy in an average size of 10 nm and completely mottled morphology.

Keywords: NanoSteel, ECAP, HPT, ARB, Melt-spinning, Glass metal, Crystallization

1- Introduction

Steel has been used by mankind for at least 3000 years and its stable position in modern society is a result of several favorable criteria including its abundant and chip raw materials (i.e. iron and coke), its recyclability, and manufacturing ability. Indeed, all kinds of steels comprise over 80% by weight of industrial metallic alloys in various forms. In other words, ferrous alloys are currently available in about 51 groups and broad area of applications [1].

The 21st is named in various aspects such as aerospace, new sources of energy, and electronic century; it is also named the century of bitter battles to gather the natural resources. Yet, nanotechnology is the newest unpredictable revolutionary science changing these names and approaches in many fields. In fact, scientists have had to resume their fundamentally beliefs within their theories because of nanoscience. Materials produced by nanotechnology can introduce a number of unbelievable mechanical and physical properties [2]. As nanotechnology flourished, some researchers presented a new theory; the era of steels will be ended up soon. In last decades, many of research focused on developing "high technology" materials with exotic properties, for example, light weight alloys (e.g. aluminum- lithium and magnesium alloys), biomaterials (e.g. high nitrogen low carbon stainless steels and cobalt- chromium alloys), shape memory alloys (i.e. nickel- titanium and copper alloys), and intermetallic alloys (e.g. Ni- Ti, Fe- Al, Ni-Al alloys) [3 and 4]. On the other hand, nanotechnology overwhelms this belief and tenders new aspects in material science. The interest toward the use of nanostructure materials arises from the fact that due to their small size of building blocks and high density of interfaces (e.g. surfaces, grains and phase boundaries) new physical and mechanical properties are expected or known from the materials. Ray of hope, nanotechnology treads in producing new kinds of ferrous alloys and opens up new approaches toward the mass production of nanostructure steels. In fact, the term "nanosteels" is called to nanostructure steels consisting of ultra-fine grains, nanosize phases (i.e. martensite, ferrite, and cementite), and nano size particles (i.e. carbides and precipitates). In other words, steels not only maintain their unique roles in modern technologies, but also may be introduced as the future materials.

In this article, producing nanostructure steels with nanosize phases and particles as well as some producing methods are discussed.

Received 2009/27/01 , Accepted 2009/14/09

[1] Faculty of Engineering, Department of Materials Science, Tarbiat Modares University, Tehran, Iran,
P.O.BOX: 14155111 **:** E-mail: Sh.Ahmadi@modares.ac.ir

[2] Corresponding author, Faculty of Engineering, Department of Materials Science, Tarbiat Modares University, Tehran, Iran

[3] Department of Material Science, Faculty of Mechanical Engineering, K. N. Toosi University of Technology, Tehran, Iran

1.1 Nanosize Phases

1.1.1 Nanosize cementite

In unalloyed steels, nanosize ferrite and pearlite are produced by ECAP (equal channel angular pressing) process. In a research, an unalloy steel was subjected to ECAP process at 623°C in 4 passes (ε=1). Results show that ultra-fine ferrite and nanosize cementite were formed in the structure. In figures 1 and 2, ferrite, pearlite and cementite in the structure are shown. In figure 3, stress-strain curves for conventional and ECAPed steel is shown. As can be seen clearly, although yield strength rises erratically after ECAP process, elongation decreases dramatically. It is known that low amount of strain hardening is the most important reason for poor elongation property [5].

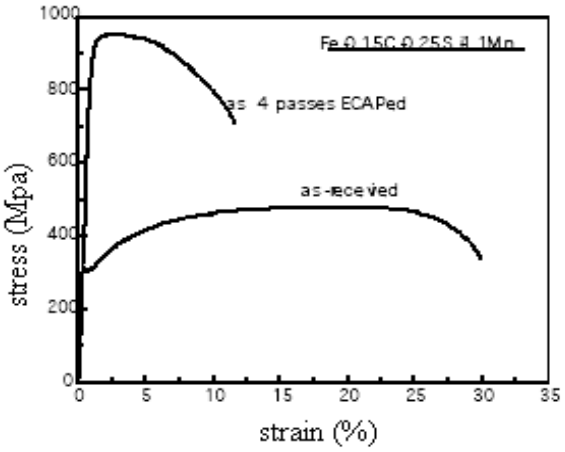

Figure 3- Stress – strain curves for the specimens before and after ECAP process [5]

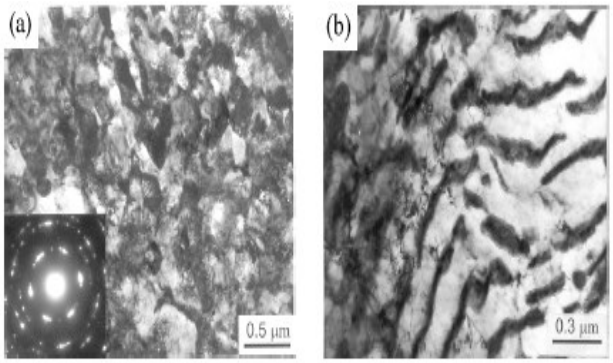

Figure 1 TEM image of a) ferrite and b) pearlite after ECAP process [5]

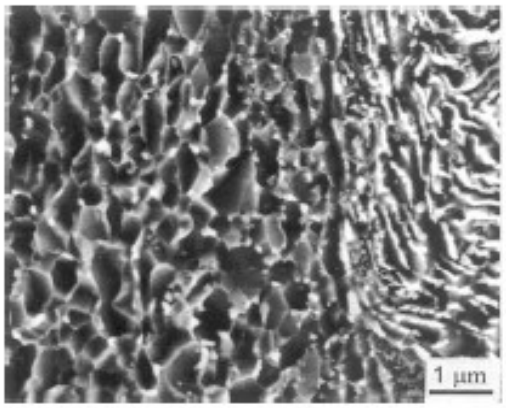

Figure 2 SEM image of nanosize cementite particles in the boundaries of ultra- fine grain ferrite [5

1.1.2 Nanosize martensite

In effect, austenitic steels (with fcc crystallographic structure) can be converted to martensite (with bcc or bct structure). In a research, converting austenite to martensite in a pre-strain 304 stainless steel was studied. In the first step, M_s temperature was determined by acoustic emission technique (about -195 K). In the second step, pre-strain specimens are cooled suddenly under this cryogenic temperature (-195 K). As shown in figure 4, structure consists of nano size martensite and remained austenite (2-100 nm) after this treatment [6].

In principle, the amount of pre-strain plays a rudimentary roll to form ultra-fine martensite. As a matter of fact, increasing pre-strain from 2% to 10% in the alloy can produce nanosize martensite instead of microsize of this after cooling treatment in cryogenic temperatures [6].

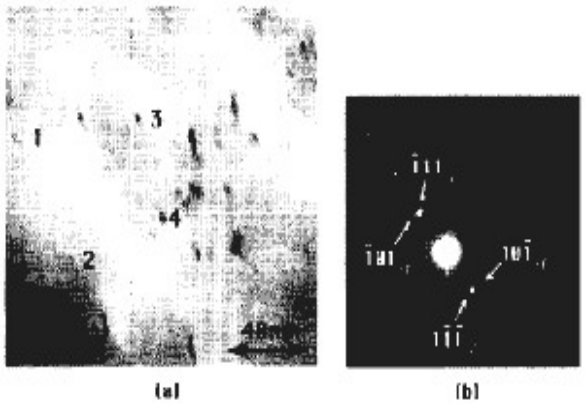

Figure 4 Bright field TEM image of nanosize martensite [6]

1.1.3 Nanosize ferrite

There are some reports about the solution of cementite and forming nanosize ferrite in unalloy (high carbon) steel during HPT (high-pressure

torsion) process. In figure 5, structure of unalloy steel subjected to HPT process with 7GPa pressure is shown. In practice, in γ=200 (γ= shear strain) the original structure is converted to submicron crystalline (SMC) structure consisting of grains with 20-50 nm diameter and 100-150 nm length. Nanosize ferrite grains (10 nm) are formed after further plastic deformation (γ=300) [7].

1.2 Nanosize carbides

1.2.1 Nanosize vanadium carbide

It is proof that nanosize vanadium carbides can be formed in low alloy steels (with 0.34 %wt V) during ECAP process and subsequent heat treatments. In a research, formation of nanosize vanadium carbides (10-30 nm) after ECAP and subsequent annealing treatment at 933 K is reported. In figure 6 ultra fine grains and nanosize carbides in low alloy steel is shown [8].

In figure 7, stress-strain curves of a low alloy steel in three deferent states (before ECAP, as ECAPed, and ECAP + annealing) are shown. The most striking feature in the chart is that a suitable combination of properties (UTS, yield strength, and elongation) can be achieved after ECAP and annealing process [8].

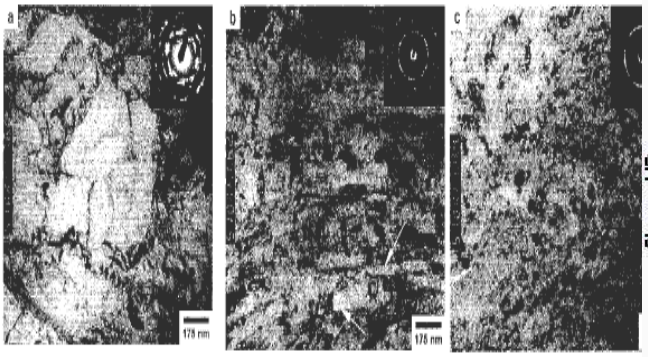

Figure 5 Bright field image and diffraction pattern the steel after HPT process [7]

1.2.2 Nanosize M_2C carbides

Formation of nanosize M_2C carbides in the structure of a martensitic stainless steel is pointed out in a patent. In particular, increasing corrosion resistance without applying any coating, increasing mechanical properties (UTS and yield strength), and enhanced elongation are the main goals in this research. The precipitate hardened stainless steel invented in this patent differs from the other kinds of steels in that the amount of chromium is limited to achieve simultaneously appropriate corrosion resistance and M_s temperature. Furthermore, nanosize (5-10 nm) M_2C and MC carbides (M= Ti, W, Cr, V) are precipitated in the structure only by multiple heat treatments. In figure 8, cyclic heat treatment to form carbides in the structure is shown [9].

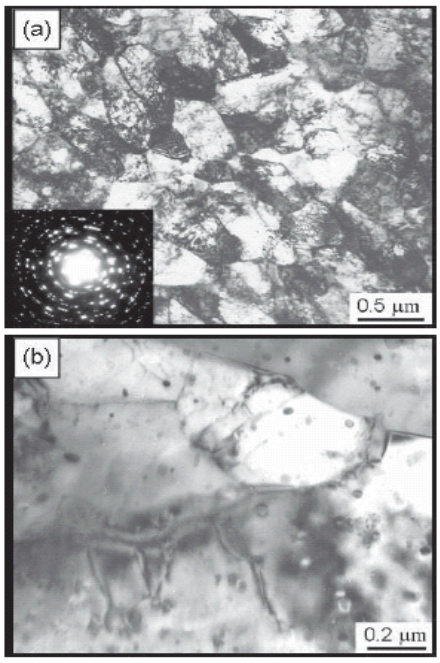

Figure 6 TEM image of a) ultra fine grain ferrite, b) nanosize vanadium carbides [8]

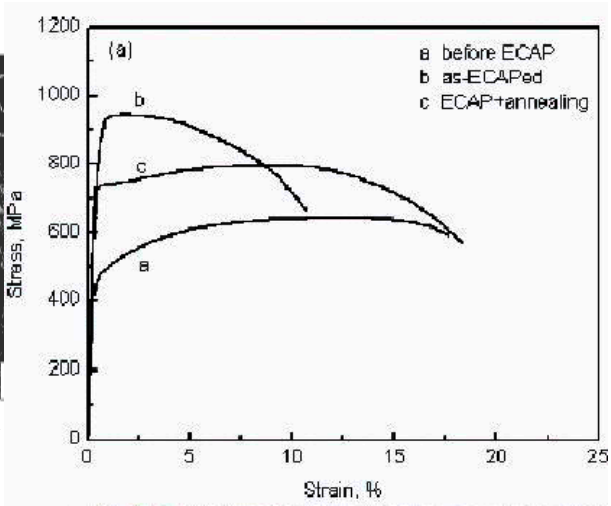

Figure 7 Stress- strain curves of vanadium alloyed steel [8]

1.3. Fabrication methods

1.3.1 SPD (Sever Plastic Deformation)

ECAP (Equal Channel Angular Pressing)

As versatile, mechanical methods have been developed allowing fabrication of nanostructure materials in large quantities with a wide rang of chemical compositions and microstructures. Among all of the severe plastic deformation techniques, equal channel angular pressing (ECAP) is especially attractive because it can economically produce bulk of ultra- fine grain (UFG) materials that are 100% dense. In fact, severe plastic deformation in ECAP

by simple shear is induced in the processing procedure by pressing the sample through a die containing two channels, equal in cross- section, and intersecting at an angle of Φ. In figure 9 a schematic picture of the process is shown. Since there is no change in the cross- sectional dimensions of the specimen, it is feasible to repeat the pressing a number of times to achieve a large degree of refined grains [6].

In a research, specimens of low alloy steel, with chemical composition according to Table 1, were subjected to ECAP process in several passes. Results showed that after 10 passes of ECAP process, microstructure was consisted of ultra-fine grains (200-300 nm). More, not only yield strength increased up to 1200 MPa but also elongation increased slightly after 4 passes of ECAP. In figure 10, microstructure of ECAPed samples are shown [10].

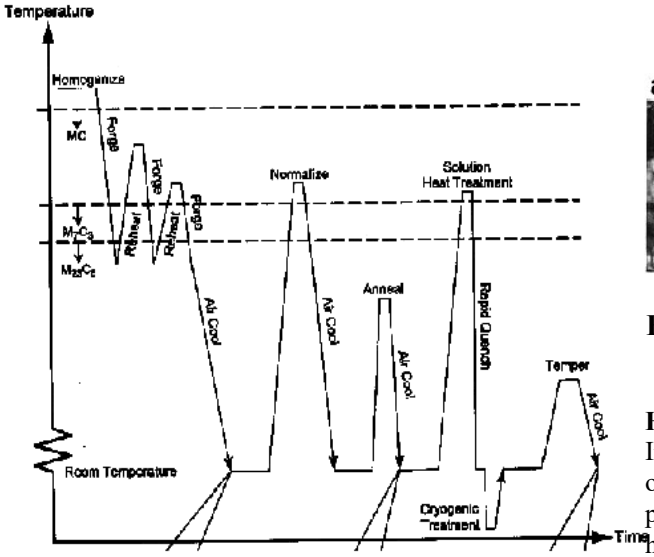

Figure 8 Multiple heat treatments to form nanosize MC and M2C carbides in a martensitic stainless steel [9].

Table 1 Chemical composition of the steel [10]

Element	Content
C	0.15
Si	0.17
Mn	0.52
P	0.019
S	0.021
Cr	0.10
Ni	0.10
Cu	0.10
Fe	Bal

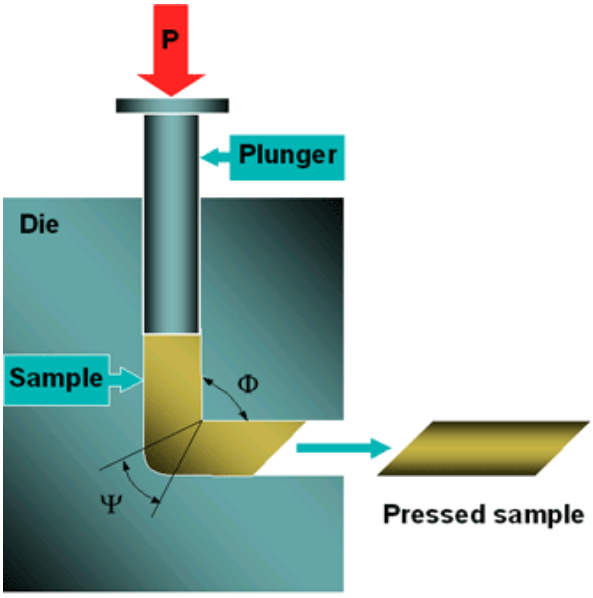

Figure 9 ECAP process

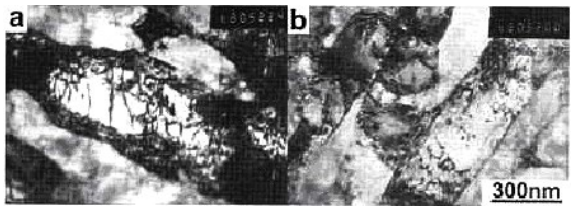

Figure 10 Microstructure of the alloy after a) 6 and b) 10 passes of ECAP process [10]

High Pressure Torsion (HPT)

In this method, a small sample (usually in the form of a disk) is simultaneously subjected to a high pressure and torsional straining. Processing by HPT has the advantage of producing exceptionally small grain sizes, often in the nanometer range (<100 nm). Nevertheless, HPT has the disadvantage that the specimen dimensions are generally fairly small, with maximum disk diameters of ~20 mm and thickness of ~1 mm. HPT process is show schematically in figure 11 [11].

In practice, small specimens of iron were subjected to HPT process to obtain ultra fine grains. In the tests, pressure was 7GPa and iron specimens were deformed under the pressure up to shear strains equal to 9, 18, 36, 181, and 363. In figure 12 microstructure of samples after HPT process in 10 rotations is shown. As can be seen clearly, ultra- fine grains (<100 nm) were formed in the structure [12].

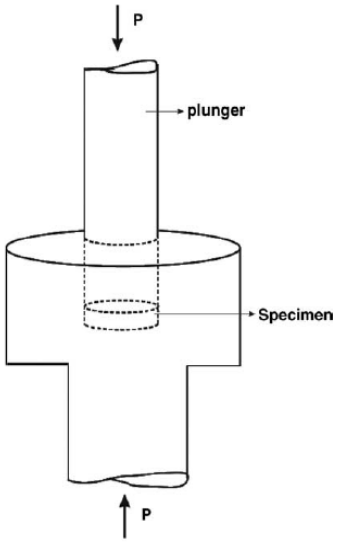

Figure 11- HPT process [11]

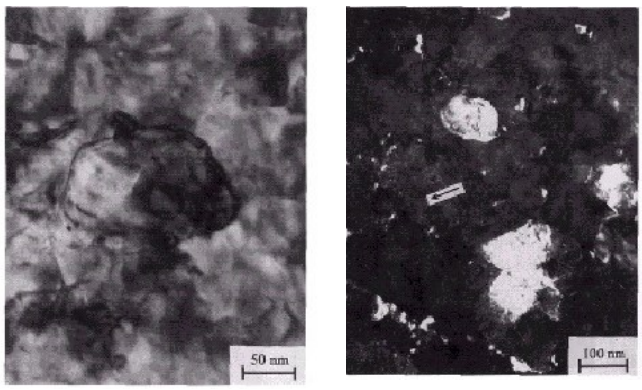

Figure 12- Microstructure f the alloy after HPT process consisting of ultra-fine grains [12]

Table 2 Chemical composition of the steel [13]

Element	Content
C	0.0031
Si	<0.01
Mn	0.15
P	0.010
S	0.005
Ti	0.049
B	0.0001
Al	0.054
Fe	Bal

Accumulative Roll Banding (ARB)

Continuous production of alloy sheets was successfully accomplished in this process. In this method, severe plastic deformation is provided by rolling sheets in several passes. Indeed, cutting rolled sheets and then rolling laminated sheets is the main technique to obtain high amount of reduction. In figure 13, ARB technique is shown [13].

In effect, specimens of a low alloy steel were successfully subjected to ARB process. Chemical composition of the steel is given in Table 2. Results showed that although tensile strength was drastically increased after several passes of ARB process, elongation was dramatically decreased instead. Fluctuation of mechanical properties for the alloy is shown in figure 14 [13].

As shown in figure 15, high volume fraction of ultra- fine grains can be formed in the structure after ARB process [13].

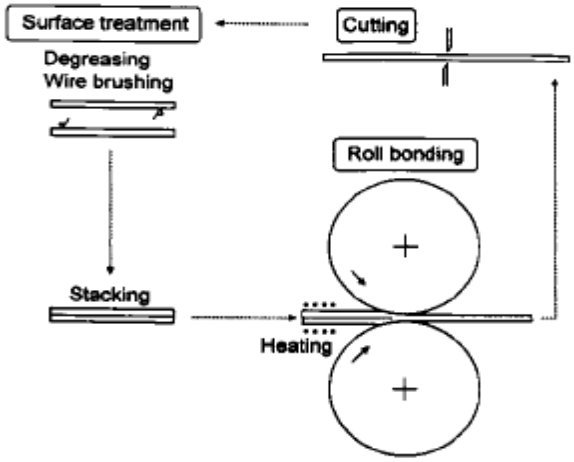

Figure 13 Accumulated roll bonding (ARB) method [13]

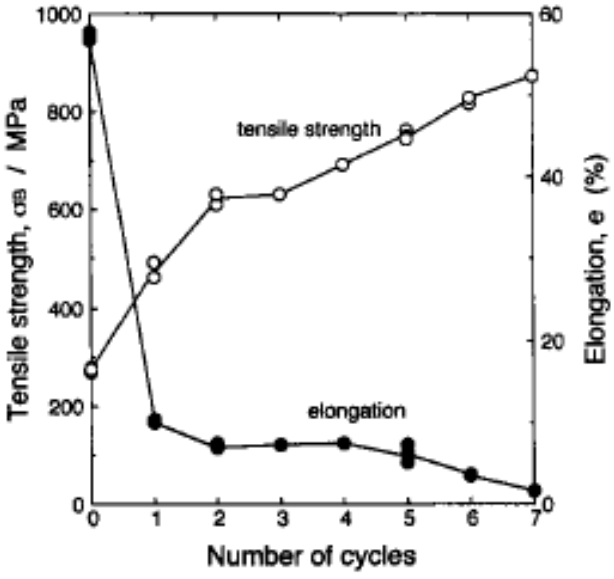

Figure 14 Mechanical properties of the alloy after different passes of ARB at 773 K [13].

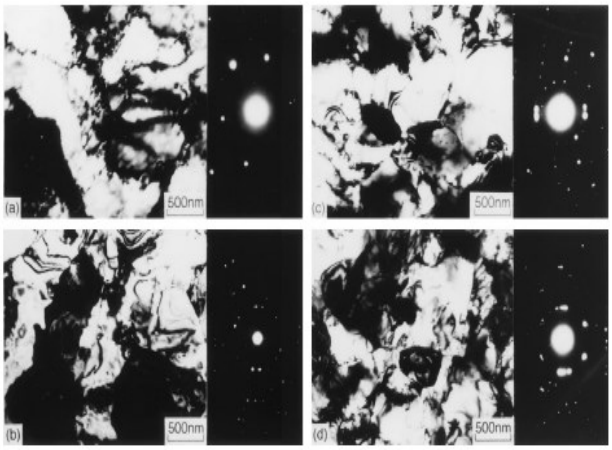

Figure 15 TEM images and diffraction pattern of the alloy specimens after a) one cycle, 50% reduction, b) 3 cycles, 87.5% reduction, c) 6 cycles, 98.4% reduction, and d) 7 cycles, 99.2% reduction [13]

1.3.2 Melt base methods

The main approach in this case is forming nanosize crystals from a steel bulk glass by controlled heat treatment. It is known that alloying with some special elements (e.g. Nb, Y) and rapid solidification from liquid state are completely necessary to form amorphous state. Although addition of alloying elements can increase GFA (glass form ability) in ferrous alloys, rapid solidification in water cooled copper molds or using melt- spinning and twin roll casting methods would be necessary to achieve amorphous structures. In practice, subsequent heat treatment is used to devitrify the glass into a nanocomposite structure consisting of nanosize crystals and phases [14, 15].

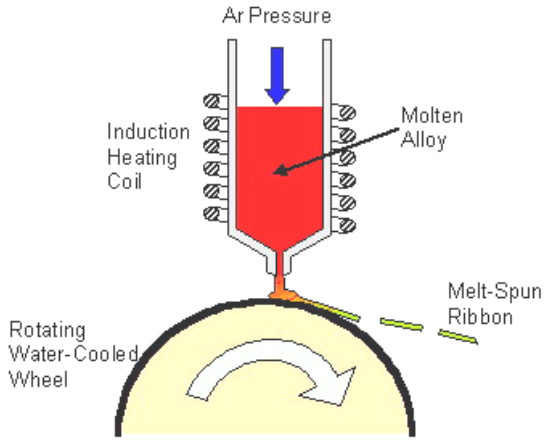

Figure 16 Melt- spinning process [16]

Melt spinning

Melt spinning is a technique used for rapid cooling of liquids (metallic or nonmetallic). In this technique, a wheel is rotated and internally cooled (usually by water or liquid nitrogen); a thin stream of liquid is then dripped onto the wheel and cooled rapidly. Thus, amorphous structures maybe form due to rapid solidification process. The cooling rates achievable by melt-spinning are on the range of 10^4–10^7 (K/s). However, the melt spinner is only able to produce small thin ribbon shaped specimens, as thin as 10 micrometers. Because of this limit, melt spinning is mainly used to produce research specimens of alloys. In figure 16, melt-spinning process is schematically shown [16 and 17].

Crystallization of melt-spun $Fe_{83}B_{17}$ metallic glass after annealing treatment was evaluated in a research work. Results showed that the metallic glass crystallizes through ultra-fine Fe-α and Fe_2B phases. Further, austenite phase formation in rapidly solidified Fe-Cr-Mn-C steels was investigated by another group of researchers. Results of this research showed that very fine austenite and ferrite were formed in the melt- spun ribbons. In figure 17, microstructure of specimens after melt-spinning is shown [18 and 19].

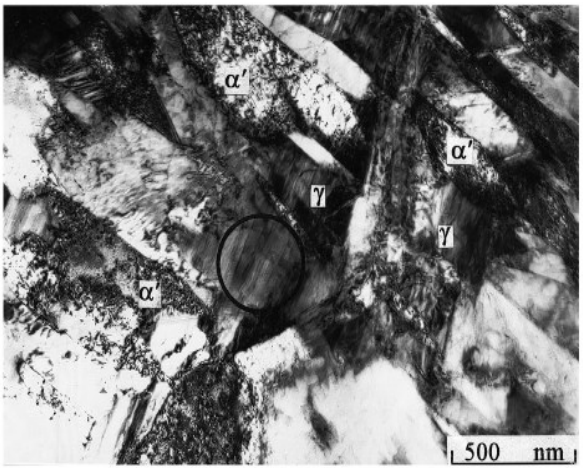

Figure 17 Microstructure of melt-spun specimens [18]

1. 4 Crystallization from amorphous state

Formation of nanosized crystals during the annealing process was named as one of the most striking features of these materials. Indeed, it is known that unstable amorphous (or glassy) structures can be devitrified to stable nanostructures by heat treating above the crystallization temperatures [20]. In effect, crystallization kinetics of melt- spun $Fe_{83}B_{17}$ and $Fe_{75}Si_9B_{16}$ metallic glass has been investigated with the aid of kinetic models such as Johnson- Mehi- Avrami (JMA) model [20, 21]. In addition, crystallization of α- Fe nano-crystals according a three- dimensional growth

model and constant nucleation rate have been suggested during heat treatments of $Fe_{81}B_{13}Si_4C_2$ alloy [22].
Generally, nucleation of crystalline phases during heat treatment and formation of nanostructure alloys have been studied by two main ways: (i) kinetic evaluations in isothermal or non- isothermal methods and (ii) microstructural evaluations by TEM or STEM. On the other hand, almost all of the attempts by Inoue and his coworkers [23, 24] about BMGs (Pd, Co, and Zr base) have been devoted to promote glass form ability (GFA). Crystallization process has been characterized in some kinds of Fe-base bulk metal glasses by D. j. Branagan and his coworkers [25, 26]. Microstructural evaluation in these kinds of BAMs showed that complex carbides e.g. $Fe_{23}(B, C)_6$ and some phases such as Fe_3B and Fe_2B were nucleated from amorphous structure after annealing process. It was also known that by nucleating of nanosize phases not only hardness and wear resistance of the alloys were promoted effectively but also abrasion and fretting resistance were enhanced drastically [27, 28].
Kinetics of crystallization process in amorphous alloys has been evaluated using DSC test and kinetic models such as Kissinger- starink, Ozawa, and Matusita. All of these models were categorized in non- isothermal analysis of crystallization in metallic glasses. Activation energy of crystallization, Avrami exponent, and growth mechanisms can be investigated using these models. In practice, characterization of crystallization process in Fe-base magnetic amorphous alloys such as $(Fe_{50}Co_{50})_{73.5}Ag_1Nb_3Si_{13.5}B_9$, $Fe_{83}B_{17}$, and $Fe_{75}Si_9B_{16}$ has been showed a diffusion controlled growth mechanism and two step crystallization process in the alloys [29-30].
In this research work, for the first time, crystallization kinetics of $Fe_{55}Cr_{18}Mo_7B_{16}C_4$ bulk amorphous alloy were evaluated using X- ray diffraction, DSC tests, and TEM observations. In fact, activation energy and types of crystallized phases were investigated during crystallization of the alloy.

2- Method and materials

Multi- component Fe- based alloy ingots were prepared in an arc furnace with nominal compositions of $Fe_{55}Cr_{18}Mo_7B_{16}C_4$. Pure iron (99.7 mass %), chromium (99.9 mass %), molybdenum (99.9 mass %), and crystalline boron (99.5 mass %) were used to produce ingots in a rod form. To achieve fully amorphous structures, rapidly solidified thin ribbons with a thickness of approximately 60 μm were prepared by melt-spinning technique (wheel speed: 32 m/s). Then, amorphous ribbons were annealed under vacuum (10^{-3} torr) in a furnace above their crystallization temperatures. X- ray diffraction (XRD) with Cu Kα radiation and differential scanning calorimetric (DSC) tests, at four different heating rates, were used to determine the crystalline phases and transformation temperatures. Composition of the ribbons was verified by using energy- dispersive X-ray spectroscopy. A 200 kV JEOL transmission electron microscope equipped with an energy dispersive X-ray spectrometer (INCA PentaFETx3 - Oxford instruments) was used to microstructural evaluations.

3- Results and discussion

3.1 Crystallization of α – Fe phase

In Figure 18, XRD pattern of $Fe_{55}Cr_{18}Mo_7B_{16}C_4$ alloy (after melt-spinning process) is shown demonstrating a broad amorphous scattering peak. No peaks corresponding to crystalline phases is indicated which means fully amorphous structure was formed in the sample after melt-spinning proce
In order to characterize the types of the crystallized phases, amorphous ribbons were annealed. In effect, temperature was chosen above the first crystallization temperature. Figure 19 shows the XRD pattern of the crystallized annealed ribbons. It is clear from the Figure 19 that α - Fe and $Fe_{23}B_5$ phases were crystallized respectively in the structure after annealing process.

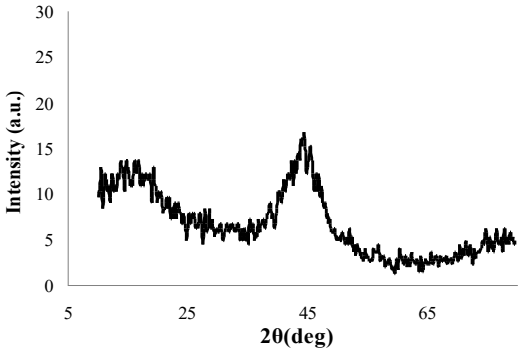

Fig 18 XRD pattern of $Fe_{55}Cr_{18}Mo_7B_{16}C_4$ in amorphous state.

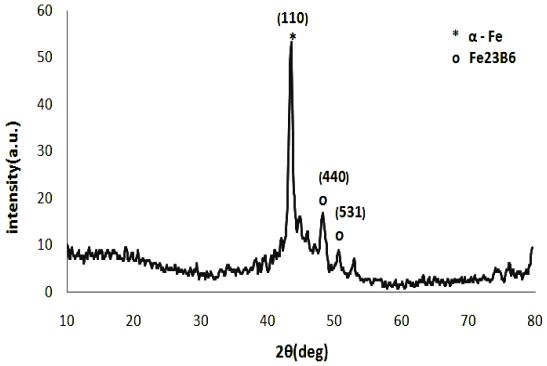

Fig 19 XRD pattern of $Fe_{55}Cr_{18}Mo_7B_{16}C_4$ alloy annealed at650°C /

3.2 TEM observations

One of the most striking features of the nanostructured Fe based alloys produced by annealing a preliminary amorphous state is the distinct appearance / morphology of the crystalline phases. For example crystalline α - Fe in the alloys forms a mottled structure; the $Fe_{23}C_6$ phase forms a featureless smooth structure [31]. In Fig. 20 microstructure of the primary alloy in amorphous state is shown. Specifically, no crystalline phases are detected in the figure.

In Fig. 21 microstructure of the crystalline alloy after heat treatment is shown in two different resolutions. It is clear from the images that crystalline α – Fe in nucleate in the amorphous structure after annealing. Indeed, complex or partially crystalline structure formed due to heat treatment above the first crystalline temperature.

Size and morphology of α – Fe crystalline phase are indicated in Fig. 22. As mentioned above, unique feature of the crystalline phases in structure of the nanostructure Fe base alloys can be effectively used toward identification of these nanosize phases. As can be seen clearly from the Figure 22, crystalline α – Fe phase nucleated in the structure an average size of 10 nm and completely mottled morphology.

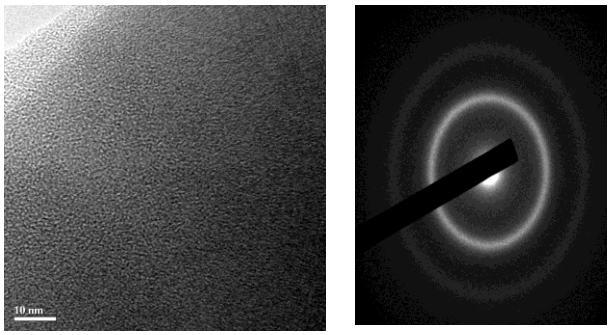

Fig 20 Microstructure of the alloy in amorphous state.

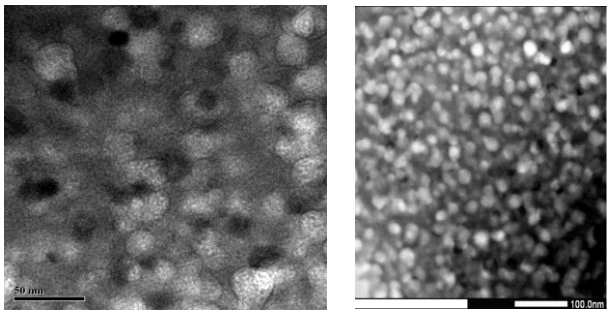

Fig 21 Microstructure of the alloy in crystalline state, a) TEM and b) STEM image.

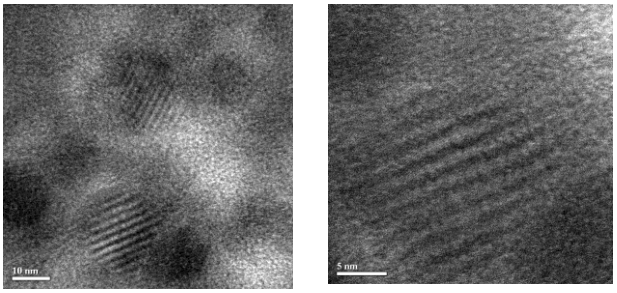

Fig 22 Crystalline α – Fe phase into the amorphous structure

4- Conclusion

Although there are many reasons to maintain steels in all industries as basic material, classifying nanosteels in high tech. material groups is due to exotic properties of nano structured steels produced by nanotechnology. It is true that nanosize phases e.g. austenite, ferrite, and cementite can be formed in the structure of steels by SPD and rapid solidification methods. Moreover, producing nanosize martensite and carbides are the most important subjects in term of "super hard" and "ultra-high strength" steels. It is important to apply appropriate fabrication methods for each group of steels to achieve nanosize phases or grains. Some of these fabrication methods consist of: ECAP, HPT, ARB, melt- spinning, and crystallization from amorphous state. From the experimental process it is known that crystalline α – Fe phase nucleated in the structure of heat treated $Fe_{55}Cr_{18}Mo_7B_{16}C_4$ alloy in an average size of 10 nm and completely mottled morphology.

References

[1] Branagan D.J., *Enabling Factors toward Production of Nanostructured Steel on an Industrial Scale*, NanoSteel Company, a report, **2008**.

[2] Branagan D.J., *The Development of Nanostructured Steel from Basic Discovery to Mainstream Technology*, NanoSteel Company, a report, **2008**.

[3] Inoue A. and Hashimoto K., Springer publication, **2001**.

[4] Sakai M. and kobayashi M., Elsevier publication, **2001**.

[5] Shin D.H. and et al., **2005**, www.msm.ac.uk

[6] Zehetbauer M.J. and Valiev R.Z., Wiley publication, **2002**.

[7] Ivanisenko Yu. V., Solid State Phenomena, Vol.94, **2003**, pp.45-50.

[8] Park K.T. and et al., Rev. Adv. Mater. Sci, **2005**, Vol.10, 133-137.

[9] US Patent 20030226625.

[10] Xang J. , C.Xu , Z.Du, Z.Zhang , L.Wang , X.Zhao .and T.G.Langdon , Proceedings of the conference ,Nanomaterials by Severe Plastic Deformation – NANOSPD2, **2002**.
[11] Meyers M.A., Mishra A., Benson D. J., Progress in materials science,vol. Vol.51, **2006**, pp.427-556.
[12] Valiev R.Z. and YU.V. Ivanisenko, E.F. Rauch and B. Baudelet, Acta mater, Vol. 44, No. 12, **1996**. pp. 4705-4712**.**
[13] Tsuji N.and et al., Scripta Mater., Vol.40, No.7, **1999**, pp. 795-800.
[14] Wang W.H. and Dong C., Material science engineering R, vol.44, **2004**, pp. 45-89.
[15] Lu Z. P., Journal of material science, Vol. 39, **2004**, pp. 3965-3974.
[16] Li Y., Journal of material science technology, Vol.15, **1999**, pp. 97-110.
[17] Telford M., Materialstoday, **2004**, pp.36-43.
[18] S. R. ChenActa materials, Vol.18, **1999**, pp.4555-4569.
[19] Soliman A.A., Thermochimica acta, vol.413, **2004**, pp. 57-62.
[20] Soliman A.A., Al-Heniti S., Al-Hajry A.and Al-Assiri M., Thermochim. Acta, Vol.413, **2004**, pp. 57-62.
[21] Chrissafi K., Maragakis M.I., Efthimiadis K. G.and Polychroniadis E. K., Alloys Compd. J. Vol.386, **2005**, pp. 165-173.
[22] Minic D.M., Maricic A. and Adnadevic B.J. Alloys Compd, Vol. 473**, 2009**, pp.363-367.
[23] Nishiyama N., Amiya K., Inoue A.and Non-Crys J., Solids, Vol.353, **2007**, pp.3615-3621.
[24] Z. Long Z., Shao Y., Xie G., Zhang P., Shen B., Inoue A. and Alloys Compd J., Vol.462, **2008**, pp.52-59.
[25] Kappes B. B., Meacham B. E., Tang Y. L.and Branagan D. J., Nanotechnology, Vol. 14, **2003**, pp. 1228-1234.
[26] Branagan D.J., Marshall M.C. and Meacham B.E, Mater. Sci. Eng. A, Vol.428, **2006**, pp. 116-123.
[27] Branagan D.J., Swank W.D., Haggard D.C., Fincke J.R. and Metal. Mater. Trans. Vol.32A, **2001**, pp. 2615- 2621.
[28] Branagan D. J., Breitsameter M., Meacham B. E., Belashchenko V. and Therm J., Spray Tech. Vol.14 **,2005**, pp.196- 204.
[29] Solima A. A., Al-Heniti S., Al-Hajry A. and Al-Assiri M., Thermochim. Acta, Vol. 413, **2004**, pp. 57-62.
[30] Chrissafi K., Maragakis M.I., Efthimiadis K.G. and Polychroniadis E.K., J. Alloys Compd. Vol.386 , **2005**, pp. 165-173.
[31] Branagan D.J., Tang Y., Appl. Sci. Manu., Vol.33, **2002**, pp. 855-859.